

Forced Nonlinear Vibrations of a One-Dimensional Bar with Arbitrary Distributions of Hysteretic Damage

Claudio Pecorari · Daniel A. Mendelsohn

Received: 8 October 2013 / Accepted: 21 January 2014 / Published online: 11 February 2014
© Springer Science+Business Media New York 2014

Abstract An analytical model is presented which predicts the forced, nonlinear response of a bar with arbitrarily distributed damage. Damage, which is either described by quadratic hysteresis, or due to dislocations interacting with point defects distributed along the dislocations' glide planes, is considered. The wave equation is solved by means of a perturbation approach. Resonance frequency shift caused by damage-induced material softening, nonlinear attenuation, and higher harmonics' generation are evaluated. For damage which is described by quadratic hysteresis, this model recovers the well-known dependence of the three acoustic quantities mentioned above on the source's strength. On the other hand, for damage due to dislocations, both frequency shift and nonlinear attenuation present a distinctive nonlinear behavior the origin of which resides in the stress dependence of the fraction of dislocations breaking away from the point defects. Furthermore, different distributions of damage having the same integrated intensity are shown to generate nonlinear effects of increasing magnitude as their spatial extent decreases. Finally, it is suggested that, once the effect of the source's strength is removed, spectral features may be used to assess the spatial extent of damage.

Keywords Nonlinearity · Hysteresis · Dislocations · Resonance

1 Introduction

Prior to fracture, material defects at atomic or mesoscopic scale multiply altering the microstructure of a material system to the extent and in a way that its response to a dynamic excitation becomes nonlinear. For this reason, interrogating a material by means of nonlinear techniques is tantamount to searching for material damage at its early stage when catastrophic failure is still a remote possibility.

Material damage often initiates and develops around localized regions containing stress concentrators. As shown in a recent theoretical investigation [1] of damage evolution, when non-local effects are accounted for, accumulation of damage is accompanied by diffusion. For these reasons, any mathematical model that aims at describing the acoustic response of a damage region at different stages of its evolution must accommodate localization and broadening of the damage spatial distribution.

Gliozzi et al. [2] used a numerical scheme to predict the nonlinear response from localized hysteretic damage. Anelastic damage was accounted for within the framework of the Preisach–Mayergoyz model in which fictitious hysteretic units are considered to exist in two states. This work showed that the dependence of the resonance frequency shift on the amplitude of the excitation is linear like in the case of uniformly distributed damage, and that different resonance modes display different sensitivity to damage localization. Interestingly, they commented on the need of deepening our understanding of the physical mechanisms responsible for the nonlinear hysteretic response as necessary condition to further develop their models and provide predictions of quantitative nature.

Van Den Abeele et al. [3] further improved the numerical approach adopting a multiscale strategy. To this end the Preisach–Mayergoyz framework was used to formulate

C. Pecorari (✉)
Hesjakollen 111 A, 5142 Bergen, Norway
e-mail: claudio.pecorari@hotmail.com

D. A. Mendelsohn
Department of Mechanical and Aerospace Engineering, The Ohio State University, 201 W. 19th Ave, Columbus, OH 43210, USA
e-mail: mendelsohn.1@osu.edu

stress–strain relationships at mesoscopic level, which were then integrated into a finite element scheme to predict the macroscopic nonlinear dynamic response of a one-dimensional bar subjected to a longitudinal excitation. They also confirmed the expected dependence of the sensitivity of various modes to the location, extent, and severity of spatially confined damage.

Windels and Van Den Abeele [4] presented the first analytical solution of the vibration problem of a one-dimensional bar affected by a confined region of damage. Damage was characterized by a cubic stress–strain constitutive relation. The solution of the time-dependent component of the wave function was found by employing a multiple time scale perturbation technique and by neglecting any effect of damage on the spatial component of the wave function. They also derived an expression for the location of the damaged region along the bar as function of the frequency shifts of two resonance modes. Van Den Abeele [5] extended this approach to tackle the problem in which the nonlinearity is of the hysteretic type with quadratic dependence on strain.

In solving the problem in which the damaged region is limited to a fraction of the bar's length, the two last references did not include any information on the location and extent of the region of damage in the constitutive relationship of the bar's material. Instead, the vibration problem was set up by assuming the bar to be uniformly damaged. A convenient consequence of this choice is the independence of the coefficients of the nonlinear terms in the wave equation from the spatial variable. Localization of damage was later introduced in the solution by evaluating certain integrals only over the region containing the damage. Although the magnitude of the error introduced by this simplification is not known, the arbitrariness of this approach by itself justifies the search of an alternative method and solution of the original problem.

Experimental results, together with both numerical and analytical models seem to indicate that the nearly linear dependence of the resonance frequency shift and of the nonlinear attenuation, together with almost the quadratic dependence of the higher harmonics' amplitude on the strength of the excitation are manifestations of non-classical nonlinearity [6]. These are the reasons which support the use of constitutive relationships containing quadratic hysteresis. At the same time, however, a variety of mechanisms have been called upon to explain possible origins of non-classical nonlinearity of both natural and man-made geomaterials, and materials with damage [7–10]. Among these, dislocations are defects affecting the material structure at its atomic level. Their dynamics continues to be a field of active research with consequences of considerable relevance for the development of nonlinear acoustic NDE (see for example [10]).

The purpose of this communication is twofold. Firstly, a recent theoretical model [11] which describes the nonlinear response of a bar subjected to a forced longitudinal, harmonic

oscillation is generalized to allow damage to be distributed arbitrarily along the bar. Secondly, this model is used to address, although to a very limited extent, the open issue concerning the link between physical mechanisms that are responsible for hysteretic damage and the nonlinear acoustic response of materials affected by the latter. To this end, two distinct forms of damage are considered. The first one is represented by a constitutive relation with the well-known quadratic hysteresis [6]. As mentioned above, it is the most commonly used constitutive relation for it reproduces trends that are typical of experimental results, and, thus, it is used here as a reference model. The second one accounts for the interaction between dislocations and point defects distributed along their dislocation's glide plane [10]. As shown in the next section, this mechanism leads to a hysteresis cycle which closely resembles the first one at low excitation's amplitude, yet its acoustic fingerprint differs from that of the former one in essential ways. The resulting wave equations for the stress field are solved by the same perturbation approach developed in [11]. Results are presented which describe the dependence of the negative shift of the resonance frequencies, the attenuation of the fundamental component, and spectral features of the nonlinear response on (i) the amplitude of the excitation, (ii) the physical nature, (iii) distribution, and (iv) location of the damage.

2 Constitutive Relations

The dynamics to be studied is caused by a source of stress applied to one of the two ends of a bar. Stress, $\sigma(x,t)$, therefore, is the physical quantity under control, while strain, $e(x,t)$, is viewed as the result of the bar's response to the applied source. In this work, as in [11], constitutive relationships expressing the dependence of strain on stress are used.

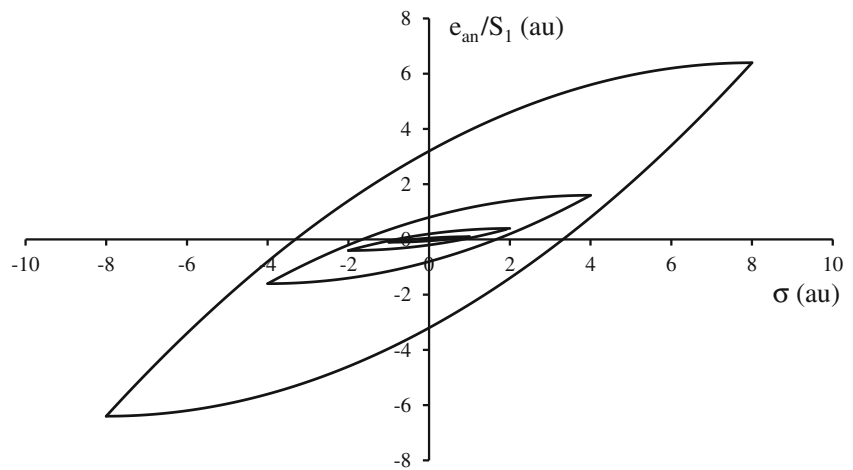
The most common constitutive relationship given in analytical form which has been used to reproduce experimental results is one in which the dependence of the anelastic response of the material on the applied stress is quadratic, and history dependent

$$e(x,t) = \int_{t_0}^t S(t-\tau)(\partial\sigma/\partial\tau)d\tau + \frac{1}{2}S_1 \left[(\sigma^2(x,t) - \sigma_{\max}^2(x)) \operatorname{sgn} \left(\frac{\partial\sigma}{\partial t} \right) + 2\sigma_{\max}(x)\sigma(x,t) \right] \quad (1)$$

In Eq. (1) the first term describes the linear viscoelastic properties of the material, and can also be written as

$$\begin{aligned} \int_{-\infty}^t S(t-\tau)(\partial\sigma/\partial\tau)d\tau &= S_0\sigma(x,t) + \int_{t_0}^t S'(t-\tau)\sigma(x,\tau)d\tau \\ &= S_0\sigma(x,t) + \int_{-\infty}^{+\infty} S'(v)\sigma(x,v)e^{-jvt}dv, \end{aligned} \quad (2)$$

Fig. 1 Anelastic strain versus stress describing quadratic hysteresis cycle in Eq. (3)



where $S_0 = S(0)$ is the elastic compliance of the material, and $S'(t - \tau)$ represents the derivative of the creep function of the material, S , with respect to its argument, and t_0 is the instant in the past when the source of vibration was switched on. The elastic compliance S_0 is the inverse of the Young Modulus E . The second equality is obtained by expressing the convolution in terms of the integral of the product of the Fourier transforms $S'(\nu)$ and $\sigma(x, \nu)$ of $S'(t)$ and $\sigma(x, t)$, respectively. The quantities S_0 and S_1 are two constants with dimensions of $[\text{stress}]^{-1}$ and $[\text{stress}]^{-2}$, while $\sigma_{\max}(x)$ is the local amplitude of the vibration and depends on Σ , the strength of the excitation source. The function $\text{sgn}(\cdot)$ is equal to 1 when its argument is positive, and to -1 when it is negative. The second term in Eq. (1) represents hysteresis. In the context offered by the interaction between elastodynamic waves and interfaces formed by rough surfaces in contact, it has been shown that friction between asperities in contact leads to boundary conditions across the interface (i.e., to an equation of state for the interface) in which stress displays a hysteretic quadratic dependence on the displacement discontinuity across the interface [12]. There seems to be no similar derivation for Eq. (1) which stems from a similarly well-defined mechanism.

Information about the spatial distribution of damage along the bar can be introduced in the constitutive relationship by multiplying the term representing hysteresis by a suitable function $U(x)$,

$$e(x,t) = S_0\sigma(x,t) + \int_{-\infty}^{+\infty} S'(\nu)\sigma(x, \nu)e^{-j\nu t}d\nu + \frac{1}{2}S_1U(x) \times \left[(\sigma^2(x,t) - \sigma_{\max}^2(x))\text{sgn}\left(\frac{\partial\sigma}{\partial t}\right) + 2\sigma_{\max}(x)\sigma(x,t) \right]. \tag{3}$$

A uniform distribution of damage along the whole extent of the bar can be represented by the function $U(x) = 1$ for all x in $[0, L]$, where L is the length of the bar. Figure 1 illustrates

a few qualitative examples of hysteresis cycles for increasing values of σ_{\max} .

Dislocations and their interaction with other microstructural features have been the focus of extensive investigations for their role in many problems concerning material science. It has been long established, for instance, that they play an important role in determining damping properties of alloys via their interaction with point defects [10]. The role of dislocations in determining the ductility of a material is also known. For this reason, a second constitutive relation is considered here which describes a material containing a distribution of dislocations interacting with point defects distributed along their glide planes. In this work, this mechanism was chosen because it leads to a macroscopic constitutive relationship similar to that in Eq. (3).

Point defects on a dislocation’s glide plane exert a pinning force on the dislocation which may be overtaken by the applied stress. The ensuing relationship between anelastic strain and stress for dislocations included in a representative volume is schematically shown in Fig. 2 [10]. This relationship assumes that all dislocations break away from their pinning defects at a critical value of the applied stress, σ_{cr} . The loading and unloading sections of the cycle comprise an initial fully plastic response followed by phases in which the anelastic strain varies linearly with stress. The cycle in Fig. 2 can be represented by the following function

$$e_{\text{an}}(x,t) = S_1H(\sigma_{\max}(x) - \sigma_{\text{cr}})C(\sigma(x,t)|\sigma_{\max}(x), \sigma_{\text{cr}}), \tag{4}$$

where $e_{\text{an}}(x,t)$ is the anelastic part of the strain field describing the deformation of the representative volume centered in x at the time t . The coefficient S_1 is a constant with dimension of $[\text{stress}]^{-1}$ which controls the slope of the linear sections of the cycle, and $H(\cdot)$ is the step function, which is equal to 1 when its argument is positive and it is null when the latter is negative. This step function ensures that no anelastic strain is

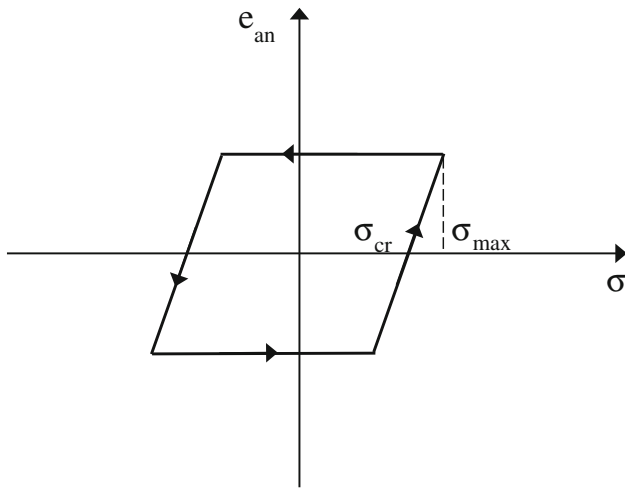


Fig. 2 Anelastic strain versus stress describing hysteresis of a representative volume containing dislocations which interact with point defects distributed along their glide plane. The symbol σ_{cr} represents the critical value of the stress at which the response of the dislocations begin to have an anelastic component

generated for values of the local amplitude σ_{max} smaller than the critical stress. The function $C(\sigma|\sigma_{max}, \sigma_{cr})$ is defined as

$$\begin{aligned}
 C(\sigma|\sigma_{max}, \sigma_{cr}) &= [(-\sigma_{max} + \sigma_{cr})H(-\sigma_{max} + 2\sigma_{cr} - \sigma) \\
 &+ (\sigma - \sigma_{cr})H(\sigma + \sigma_{max} - 2\sigma_{cr})]H(\dot{\sigma}) \\
 &+ [(\sigma_{max} - \sigma_{cr})H(\sigma - \sigma_{max} + 2\sigma_{cr}) \\
 &+ (\sigma + \sigma_{cr})H(\sigma_{max} - 2\sigma_{cr} - \sigma)]H(-\dot{\sigma}). \tag{5}
 \end{aligned}$$

In Eq. (5), the symbol $\dot{\sigma} = \partial\sigma/\partial t$. Furthermore, the first and third term of the RHS represent the fully plastic sections of the cycle, while the second and fourth one represent the linear loading and unloading, respectively.

It seems reasonable to assume that different dislocations may break away from the point defects with which they interact at different values of the critical stress σ_{cr} . To account for this material property, a probability density function, $\varphi(\sigma_{cr})$, can be used to represent the fraction of dislocations in the representative volume which break away at values of the stress between σ_{cr} and $(\sigma_{cr} + d\sigma_{cr}) : \varphi(\sigma_{cr})d\sigma_{cr}$. Therefore, the dependence of the average anelastic macroscopic strain from stress can be obtained by evaluating the following integral

$$\begin{aligned}
 e_{an}(x,t) &= S_1 \int_0^{\sigma_{max}} H(\sigma_{max} - \sigma_{cr})C(\sigma|\sigma_{max}, \sigma_{cr})\varphi(\sigma_{cr})d\sigma_{cr}. \tag{6}
 \end{aligned}$$

Using the probability density function $\varphi(\sigma_{cr})$

$$\varphi(\sigma_{cr}) = \frac{\sigma_{cr}}{\Delta^2} e^{-\sigma_{cr}/\Delta} \tag{7}$$

the integral in the RHS of Eq. (6) can be evaluated analytically. The quantity Δ in Eq. (7) controls the width of the distribution, and is the only additional parameter introduced in this model. Its value measures the strength of the interaction between dislocations and point defects, and, therefore, it depends also on the physical nature of the latter. The choice of the function in Eq. (7) to describe the distribution of σ_{cr} is dictated by only two criteria. The first one is that there is an upper, yet unknown limit of the stress above which all dislocations break free from their pinning points. This property translates into having a distribution that decays exponentially with increasing σ_{cr} . The second criterion concerns the fact that, in general, work has to be done to free any dislocation from its pinning point defects. Therefore, it can be reasonably assumed that, in the limit of σ_{cr} becoming smaller and smaller, even the number of dislocations breaking free at this level of stress decreases accordingly. This property is accounted for by the exponential's pre-factor, which goes to zero as σ_{cr} . The result is

$$\begin{aligned}
 e_{an}(x,t) &= S_1 U \left\{ [\sigma - (\sigma_{max} + \sigma)(1 + z_+)e^{-z_+} \right. \\
 &+ \sigma_{max}(1 + z_0)e^{-z_0} 2\Delta(1 - 2(1 + z_+ + z_+^2/2))e^{-z_+} \\
 &+ (1 + z_0 + z_0^2/2)e^{-z_0}] H(\dot{\sigma}) + [\sigma + (\sigma_{max} - \sigma) \\
 &\times (1 + z_-)e^{-z_-} - \sigma_{max}(1 + z_0)e^{-z_0} \\
 &+ 2\Delta(1 - 2(1 + z_- + z_-^2/2))e^{-z_-} \tag{8}
 \end{aligned}$$

In Eq. (8), $z_{\pm} = (\sigma_{max} \pm \sigma)/(2\Delta)$, $z_0 = \sigma_{max}/\Delta$, and the function $U = U(x)$, similarly to Eq. (3), defines the spatial distribution of damage along the bar. Furthermore, it is stressed again that, while S_1 plays identical roles in Eqs. (1) and (3), the physical dimensions of this quantity are not the same in the two cases. Figure 3 offers examples of this hysteresis cycle for four different values of σ_{max} assuming that $\Delta = 1$ if measured by the same unit as σ . Comparison between Figs. 1 and 3 indicates that the area of the former increases faster than that of the latter as σ_{max} increases.

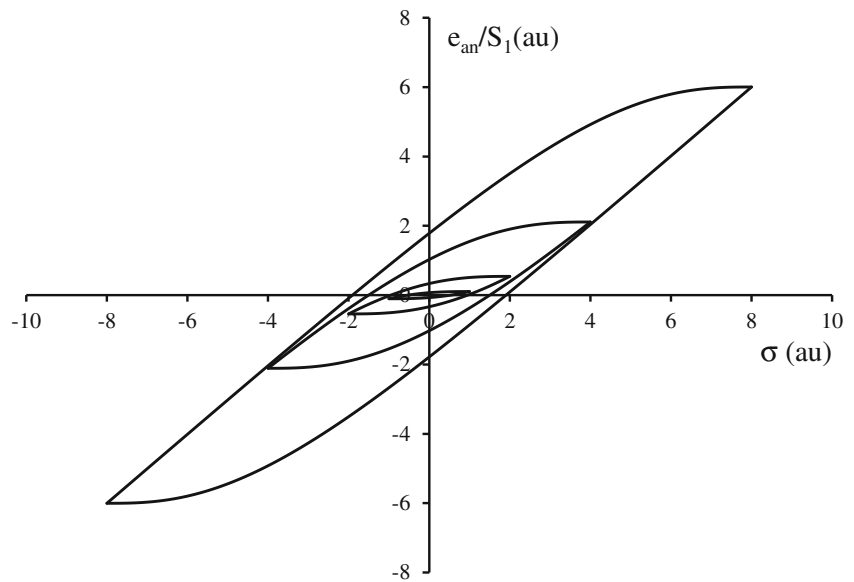
3 Equation of Motion

The two constitutive relationships presented in the previous section can be written in a shorter notation as

$$\begin{aligned}
 e(x,t) &= S_0\sigma(x,t) + \int_{-\infty}^{+\infty} S'(v)\sigma(x,v)e^{-jvt}dv \\
 &+ S_1U(x)\Gamma(x,t|\sigma, \sigma_{max}, \dot{\sigma}), \tag{9}
 \end{aligned}$$

the function $\Gamma(x,t|\sigma, \sigma_{max}, \dot{\sigma})$ representing the anelastic component of the total strain given in Eqs. (3) and (8). Introducing Eq. (9) in the equation of motion for the stress field yields

Fig. 3 Anelastic strain versus stress (Eq. 8) for a material with dislocations interacting with point defects distributed along their glide planes



$$\frac{\partial^2 \sigma(x,t)}{\partial x^2} = \rho \frac{\partial^2}{\partial t^2} \left\{ S_0 \sigma(x,t) + \int_{-\infty}^{+\infty} S'(\nu) \sigma(x,\nu) e^{-j\nu t} d\nu + S_1 U(x) \Gamma(x,t | \sigma, \sigma_{\max}, \dot{\sigma}) \right\}, \quad (10)$$

Equation (10) has to be solved with the following boundary conditions

$$\sigma(x = 0, t) = \Sigma e^{-j\omega t}, \quad (11a)$$

$$\sigma(x = L, t) = 0. \quad (11b)$$

Let the total stress field $\sigma(x,t)$ be written as the sum of two functions $\sigma_0(x,t|\varepsilon)$ and $\sigma_1(x,t|\varepsilon)$, where ε is a small parameter to be specified later

$$\sigma(x,t) = \sigma_0(x,t|\varepsilon) + \sigma_1(x,t|\varepsilon). \quad (12)$$

In Eq. (12), $\sigma_0(x,t|\varepsilon)$ is a function which coincides with the solution of the linear problem when $\varepsilon = 0$, while $\sigma_1(x,t|\varepsilon)$ vanishes in the same limit. The dependence of $\sigma_0(x,t|\varepsilon)$ on ε accounts for the softening of the material caused by damage, while $\sigma_1(x,t|\varepsilon)$ results from the generation of higher harmonics and nonlinear attenuation. Furthermore, the norm of σ_0 is much greater than that of σ_1 , $\|\sigma_0\| \gg \|\sigma_1\|$, for any values of the parameter ε . Let $\Sigma_0 = \max[\sigma_0(x,t|\varepsilon)]$ for every $x \in [0, L]$, and at any time t , and introduce the new normalized field function

$$\xi(x,t) = \xi_0(x,t|\varepsilon) + \xi_1(x,t|\varepsilon), \quad (13)$$

where $\xi = \sigma/\Sigma_0$, $\xi_0 = \sigma_0/\Sigma_0$, and $\xi_1 = \sigma_1/\Sigma_0$, by virtue of which the amplitude of $\xi_0(x,t|\varepsilon)$ is never larger than 1 along

the bar. Introducing Eq. (13) into the equation of motion, Eq. (10) yields the following equation

$$\frac{\partial^2}{\partial x^2} [\xi_0(x,t) + \xi_1(x,t)] = \rho \frac{\partial^2}{\partial t^2} \left\{ S_0 [\xi_0(x,t) + \xi_1(x,t)] + S_1 U(x) \Gamma(x,t | (\xi_0 + \xi_1), (\xi_0 + \xi_1)_{\max}, (\dot{\xi}_0 + \dot{\xi}_1)) + \int_{-\infty}^{+\infty} S'(\nu) [\xi_0(x,\nu) + \xi_1(x,\nu)] e^{-j\nu t} d\nu \right\} \quad (14)$$

Using the inequality $\|\xi_0\| \gg \|\xi_1\|$, Eq. (14) can be split into two equations governing the spatial and time evolution of ξ_0 and ξ_1 , respectively. They are

$$\frac{\partial^2 \xi_0}{\partial x^2} = \rho \frac{\partial^2}{\partial t^2} \left[S_0 (1 + \varepsilon \gamma(x)) \xi_0 + \int_{-\infty}^{+\infty} S'(\nu) \xi_0(x,\nu) e^{-j\nu t} d\nu \right], \quad (15a)$$

$$\frac{\partial^2 \xi_1}{\partial x^2} = \rho \frac{\partial^2}{\partial t^2} \left[S_0 (1 + \varepsilon \gamma(x)) \xi_1 + \int_{-\infty}^{+\infty} S'(\nu) \xi_1(x,\nu) e^{-j\nu t} d\nu \right] + \varepsilon \rho S_0 U(x) \frac{\partial^2}{\partial t^2} \Gamma'(x,t | \xi_0, \xi_{0,\max}, \dot{\xi}) \quad (15b)$$

In Eq. (15a), $\varepsilon = \Sigma_0(S_1/S_0)$, and $\gamma(x) = \xi_{0,\max}(x)U(x)$ for the case of quadratic hysteresis, while $\varepsilon = (S_1/S_0)$, and $\gamma(x) = U(x) [1 - (1 - z_0(x)/2)e^{-z_0(x)/2}]$ for a distribution of dislocations. Recall that $z_0(x) = \sigma_{\max}(x)/\Delta$. Note that, in both equations, the inclusion of $\varepsilon \gamma(x)$ in the coefficient of the first second-order derivative of the unknown function allows the solution to account for the effect of damage-induced material softening. This term derives from the definition of the function Γ . Thus, new function Γ' on the RHS of Eq. (15b) is obtained by subtracting $\rho S_0 \varepsilon \gamma(x) \xi_1$ from Γ .

Finally, the argument of Γ' has been approximated by substituting ξ with ξ_0 in view of the fact that the error introduced in this way is an order of magnitude smaller than $\|\xi_1\|$.

For the way ξ_0 and ξ_1 have been defined, Eq. (15a) has to be solved together with the boundary conditions derived from Eq. (11a, 11b) once the stress field has been normalized by the constant Σ_0 . On the other hand, the boundary conditions associated with Eq. (15b) require the normalized stress field ξ_1 to be null at both ends of the bar, $\xi_1(x = 0) = \xi_1(x = L) = 0$.

Equation (15a) is nonlinear since the coefficient of $(\partial^2 \xi_0 / \partial t^2)$ depends on the solution itself through $\gamma(x)$. To circumvent this difficulty, $\gamma(x)$ can be written as the sum of its mean value over the bar, which is independent of x , and a new function $\Delta\gamma(x)$, $\gamma(x) = \langle \gamma \rangle(x) + \Delta\gamma(x)$, so that Eq. (15a) can be rearranged as follows

$$\frac{\partial^2 \xi_0}{\partial x^2} - \rho \frac{\partial^2}{\partial t^2} \left[S_0(1 + \varepsilon \langle \gamma(x) \rangle) \xi_0 + \int_{-\infty}^{+\infty} S'(v) \xi_0(x, v) e^{-jvt} dv \right] = \rho S_0 \varepsilon \Delta\gamma(x) \frac{\partial^2 \xi_0}{\partial t^2}. \tag{16}$$

The original equation has been transformed in such a way that its homogeneous version has the form of a linear integro-differential equation which is affected by damage through the average value of the latter over the bar. The RHS of this equation, which depends on the damage location, plays the role of a source contributing to the general solution with a correction of the first order in ε . This consideration suggests searching for an approximate solution of Eq. (17) by writing $\xi_0 = \xi'_0 + \xi''_0$, where the former term is the solution of the homogeneous equation

$$\frac{\partial^2 \xi'_0}{\partial x^2} - \rho S_0 \frac{\partial^2}{\partial t^2} \left[(1 + \varepsilon \langle \gamma(x) \rangle) \xi'_0 + j \int_{-\infty}^{+\infty} \eta(v) \xi'_0(x, v) e^{-jvt} dv \right] = 0, \tag{17}$$

with boundary conditions $\xi'_0(x = 0, t) = (\Sigma / \Sigma_0) e^{-j\omega t}$, and $\xi'_0(x = L, t) = 0$, while the second term is found solving the following equation

$$\frac{\partial^2 \xi''_0}{\partial x^2} - \rho S_0 \frac{\partial^2}{\partial t^2} \left[(1 + \varepsilon \langle \gamma(x) \rangle) \xi''_0 + j \int_{-\infty}^{+\infty} \eta(v) \xi''_0(x, v) e^{-jvt} dv \right] = \rho S_0 \varepsilon \Delta\gamma(x) \frac{\partial^2 \xi'_0}{\partial t^2}, \tag{18}$$

with boundary conditions $\xi''_0(x = 0, t) = \xi''_0(x = L, t) = 0$. Note that the substitution of ξ_0 with ξ'_0 in the RHS of Eq. (18) is justified by the fact that they are of the same order of magnitude. In Eqs. (17) and (18), $j\eta(v) = S'(v)/S_0$, where j is

the imaginary unit, is responsible for the linear attenuation experienced by the stress field. A complete model of the viscoelastic behavior of the material should include also a real component in $S'(v)$. Given that the vibrations of the bar are forced by a harmonic source with frequency ω , the introduction of $\text{Re}[S'(v)]$ would alter only the value of the material compliance at the frequency of the excitation, leaving the nonlinearity of the material unaffected.

The boundary conditions enforced on the solution of Eq. (17) require that the Fourier transform of the normalized stress $\xi'_0(x, v)$ to be proportional to $\delta(v - \omega)$: $\xi'_0(x, v) = \xi'_0(x) \delta(v - \omega)$. This observation greatly simplifies Eq. (17), which can thus be written as

$$\frac{\partial^2 \xi'_0}{\partial x^2} + \rho \omega^2 S_0 [(1 + \varepsilon \langle \gamma(x) \rangle) + j\eta(\omega)] \xi'_0 = 0. \tag{19}$$

This equation governs the longitudinal vibrations of a bar with effective compliance given by $S_0[(1 + \varepsilon \langle \gamma(x) \rangle) + j\eta(\omega)]$. Note that being $\varepsilon \langle \gamma(x) \rangle$ positive, the effect of nonlinear hysteresis is to soften the material regardless whether the applied stress is compressive or tensile. Further, through the link between the linear attenuation coefficient, α , and the linear quality factor, Q_{Lin} , one can identify $\eta(\omega)$ as the inverse of Q_{Lin} . To obtain Eq. (19), the time dependence of the solution has been assumed to be that of the source, $e^{-j\omega t}$. The solution of this nonlinear homogeneous equation is found by iteration, assuming as a seed of this process the solution of the linear problem

$$\xi'_{lin}(x, t) = \frac{\Sigma}{\Sigma_0} \frac{\sin[k_{lin}(x - L)]}{\sin(k_{lin}L)} e^{-j\omega t}, \tag{20}$$

where $k_{lin}^2 = \rho S_0 [1 + j\eta(\omega)] \omega^2$. This function is used to evaluate $\langle \gamma(x) \rangle$ first, and then the new solution ξ'_0 , which has the same analytic form as ξ'_{lin} . The iteration continues until convergence of $k^2 = \rho S_0 [(1 + \varepsilon \langle \gamma(x) \rangle) + j\eta(\omega)] \omega^2$ is achieved.

This solution is employed to evaluate the source function of Eq. (18), with which the solution of that equation is found to be

$$\xi''_0(x, t) = \rho S_0 \varepsilon \int_0^L \Delta\gamma(x') \frac{\partial^2 \xi'_0}{\partial t^2} G(x, x') dx' e^{-j\omega t}, \tag{21}$$

where $G(x, x')$ [11] is the Green function which describes the vibration due to a point source at x' , and satisfies the boundary conditions $G(0, x') = G(L, x') = 0$. These boundary conditions render the solution of the homogeneous wave equations for $\xi''_0(x, t)$ identically null within $[0, L]$. Furthermore, they must be satisfied by $\xi''_0(x, t)$ since $\xi'_0(x, t)$, by itself, satisfies those enforced on the total field.

Considerations identical to those just examined can be used to solve Eq. (15b). In fact, even in this case the bound-

ary conditions which accompany this equation lead to the conclusion that the solution of the homogeneous equation derived from Eq. (15b) is identically null over [0, L]. To solve the Eq. (15b), the harmonic balance method is employed. To this end, the source function is expanded in a Fourier series of harmonics with frequencies that are multiples of that of the applied source,

$$U(x) \frac{\partial^2}{\partial t^2} \Gamma'(x, t | \xi_0, \xi_{0, \max}, \dot{\xi}_0) = \sum_{n=-\infty}^{+\infty} F_n(x) e^{-jn\omega t}. \quad (22)$$

Using this representation of the source function, and the harmonic balance method, Eq. (15b) leads to a series of equations, the n-th of which yields the n-th harmonic component of ξ_1

$$\xi_{1, n}(x, t) = \varepsilon \rho S_0 \int_0^L F_n(x') G_n(x, x') dx' e^{-jn\omega t}. \quad (23)$$

Of these components, $\xi_{1, 1}(x, t)$ accounts for most of the attenuation experienced by the fundamental component. In Eq. (23), the Green's function $G_n(x, x')$ [11] represents the vibration generated by a point source with harmonic time dependence characterized by the frequency $\omega_n = n\omega$, radiating in a medium with effective compliance $S_0[(1 + \varepsilon \langle \gamma(x) \rangle) + j\eta(\omega)]$.

To recover strain from stress, the nonlinear constitutive relationship in Eq. (9) should be used. To the order of approximation adopted in this work, however, the inclusion of the nonlinear terms amounts to a correction in the fourth significant digit, which can be neglected. For this reason, once the stress field accounting for nonlinear effects up to the first order correction in ε is known, any dependence on the magnitude of the source which can be attributed to the stress field can also be considered as a characteristic of the displacement field, and thus, of the velocity and acceleration of any material point along the bar.

4 Numerical Results

In this section, numerical results are presented which refer to a material with mechanical properties similar to those of Berea Sandstone with mass density $\rho = 2.077 \cdot 10^3 \text{ kg/m}^3$, and Young's Modulus $E = 15 \text{ GPa}$. Dissipation is controlled by the non-dimensional function $\eta(\omega)$ which, in this simulation, is assumed to be frequency independent and equal to $\eta(\omega) = 10^{-2}$. Note that this assumption yields a linear wave number with imaginary part proportional to ω . The constants S_1 is numerically equal to $5 \cdot 10^{-10} S_0$ in the model of the quadratic hysteresis cycle (Eq. 3), while $S_1 = 5 \cdot 10^{-4} S_0$ in Eq. (8). In this work, the constant Δ in Eq. (7) controlling the width of the distribution of σ_{cr} is equal to 30 kPa. With this value

of Δ , the probability density function extends to values of σ_{cr} up to 200 kPa. In principle, the nonlinear response of a material should be expected to be sensitive to the value of Δ . The choice of $\Delta = 30 \text{ kPa}$ has been made in view of the agreement obtained between a model based on Eq. (8) and experimental results [13] in a theoretical investigation of the physical origins of the dynamic acoustic response on Berea sandstone [14]. Finally, the length of the bar is $L = 0.3 \text{ m}$.

In the following, the effect of the nature of damage is investigated first. In these simulations, the function which describes the distribution of damage along the bar is assumed to be equal to 1 along the whole bar, i.e., $U(x) = 1, \forall x \in [0, L]$. The effect of changing $U(x)$ is examined afterwards.

A final comment is in order to warn the reader not to regard the quantitative difference between the two models as meaningful. They depend on the magnitude of the constant S_1 the physical dimensions of which are different in the two models of damage. Therefore, any comparison between the two is not straightforward. On the other hand, qualitative differences in the dependences among the physical and acoustic parameters are relevant.

4.1 Uniform Distribution

One of the main features which have been regarded as manifestation of non-classical nonlinearity is the dependence of the resonance frequency, ω_R , on the amplitude of the vibration.

Numerous publications have reported results showing an essentially linear dependence of the frequency shift $\Delta\omega_R = \omega_R - \omega_{Lin}$, where ω_{Lin} is the resonance frequency in the linear regime, on some system parameter connected to the amplitude of the source, Σ . In this work, the resonance frequency has been determined as the frequency at which the resonance curve of the stress field attains its maximum. Indeed, Fig. 4 shows that the model presented in the previous section reproduces the expected linear behavior if damage is represented by quadratic hysteresis. These data points have been generated assuming the bar being excited in the neighborhood of its first resonance. The frequency ω_0 which is used as normalization constant for $\Delta\omega_R$ is $\omega_0 = \pi / (L \sqrt{\rho S_0})$, which is the first resonance of a bar of length L , of the same material but without dissipation. On the other hand, the data calculated for a bar with a distribution of dislocations interacting with point defects distributed along the dislocations' glide planes appear to display a markedly nonlinear trend. This behavior may be understood in terms of the dependence of the fraction of dislocations which break away from surrounding point defects. For values of Σ smaller than Δ the increase of the number of dislocations breaking away from point defects along the whole length of the bar leads to a seemingly linear dependence of $\Delta\omega_R$ on the source's strength. As Σ increases further, the central region of the bar becomes subjected to such

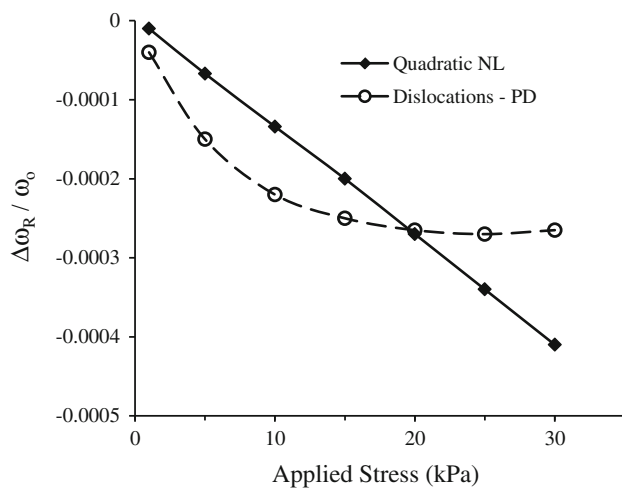


Fig. 4 Relative frequency shift as functions of the strength of the vibration source. Two bars which are affected by quadratic hysteresis (*square black symbols*) and dislocations interacting with point defects (*white circles*) are considered

a high stress that all the dislocations in that region break free, and any further increase of Σ no longer affects the behavior of the bar in that region. The extent of this region, however, continues to grow with increasing Σ , leading to a further reduction of the resonance frequency of the fundamental harmonic component. At values of the applied stress so high that no dislocation is still pinned to the surrounding point defects, any further increase of Σ produces no additional change in $\Delta\omega_R$.

A second acoustic parameter which has been used to detect and monitor damage evolution is the inverse of the quality factor, Q . When damage affects the response of a material, this quantity appears to increase proportionally to the amplitude of the excitation. Experimentally, Q may be determined by the width of a resonance curve, the identification of which is the result of an ad hoc fitting procedure, especially if the resonance curve suffers high distortion caused by nonlinearity. In this work, an approach similar to the so-called scaling subtraction method developed by Scalerandi et al. [15] and Bruno et al. [16] is adopted instead. By this method, the signal obtained by subtracting a scaled version of the linear response from the actual signal is decomposed in three parts, one of them being the relative variation of the amplitude of the fundamental component at the excitation's frequency. The scaling factor is determined by the ratio, Σ , between the amplitude of the current excitation, Σ , and of one for which the material's response is linear, Σ_{Lin} : $\kappa = \Sigma / \Sigma_{Lin}$. Figure 5 illustrates a number of data points which have been evaluated for the two types of damage and increasing values of Σ . Note the maximum value attained by the relative amplitude variation of the stress field vibrating a bar with dislocation-induced damage, as predicted also in [10]. The excitation frequency has been assumed to be $\omega_0 = \pi / (L\sqrt{\rho S_0})$. Identical remarks

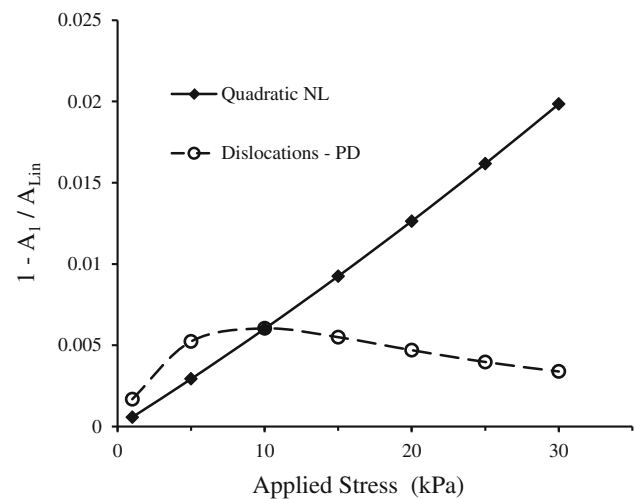


Fig. 5 Relative variation of the amplitude of the fundamental component as functions of the strength of the vibration source. Two bars are considered, which are affected by quadratic hysteresis (*square black symbols*) and dislocations interacting with point defects (*white circles*)

to those made about the previous figure apply here. Renaud et al. [14], have recently presented experimental results which, although only over a limited range that corresponds to values of $\sigma \leq 10$ kPa in Fig. 5, follow the general trend of those associated with the interaction between dislocation–point defects in Fig. 5. The results in Fig. 5 referring to damage involving dislocation distributions may also be understood as the result of two competing effects: the increase of energy stored in the fundamental component, on one side, and the increasing fraction of dislocations which break free from their pinning defects, on the other. As the former increases linearly with the strength of the source, the latter grows even faster at the beginning to become progressively less and less relevant as the remnant fraction of dislocations, which are still pinned, decreases. In this instance the choice of function in Eq. (7) matters.

In conclusion, the results in Figs. 4 and 5 provide evidence which, in principle, may be used to discriminate these forms of damage from each other, and demonstrates that damage leading to hysteresis may yield dependences of nonlinear attenuation and resonance frequency shift on the excitation's strength that are not linear.

Equation (23) provides the way to evaluate the normalized amplitudes of the higher harmonics. Recovering the explicit expression for the coefficients $F_n(x)$ (see also [11] for the case of quadratic hysteresis) brings out the quadratic dependence of the higher harmonics on the amplitude of the excitation. Figure 6 offers a comparison between the first five higher harmonics generated by two uniform distributions of damage considered in this work. The amplitude and the frequency of the excitation are $\Sigma = 15$ kPa and $\omega = \pi / (L\sqrt{\rho S_0})$, respectively. As expected from the similarity of the hysteresis cycles, the associated spectra display no remarkable

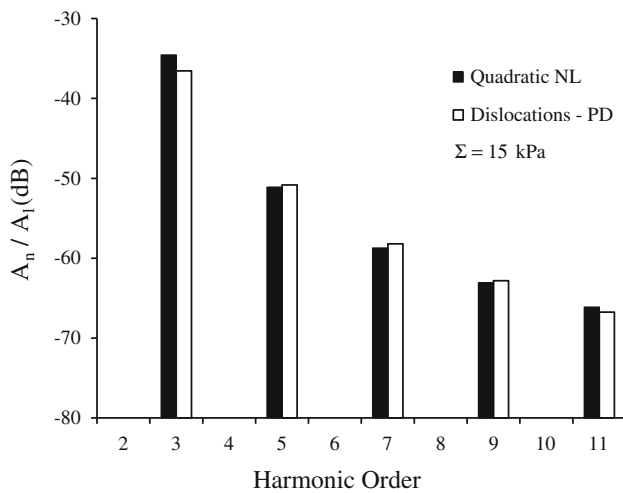


Fig. 6 Spectra generated by two uniform distributions of damage described by a quadratic hysteresis (*black bars*), and by of dislocations interacting with point defects (*white bars*). The amplitude of the source is $\Sigma = 15$ kPa

feature that may be used to discriminate the two from each other. In particular, both contain odd harmonics only. Furthermore, in agreement with the findings by Bruno et al. [16], the energy spent to generate higher harmonics can be estimated as being at least one order of magnitude smaller than the energy loss due to nonlinear attenuation. Finally, the increasing gap between the two models in Fig. 5 can be correlated to a comparison by Riviere et al. [17] between the dependence of the material’s modulus defect on the source strength and predictions based on the quadratic hysteresis damage. These authors found the latter to be incompatible with the experimental evidence because it grossly overestimates the variations of the modulus defect. On the contrary, recent theoretical results have demonstrated that a model based on Eq. (8) can account for both the offset of the modulus defect and the magnitude of the areas defined by the hysteresis cycle [13].

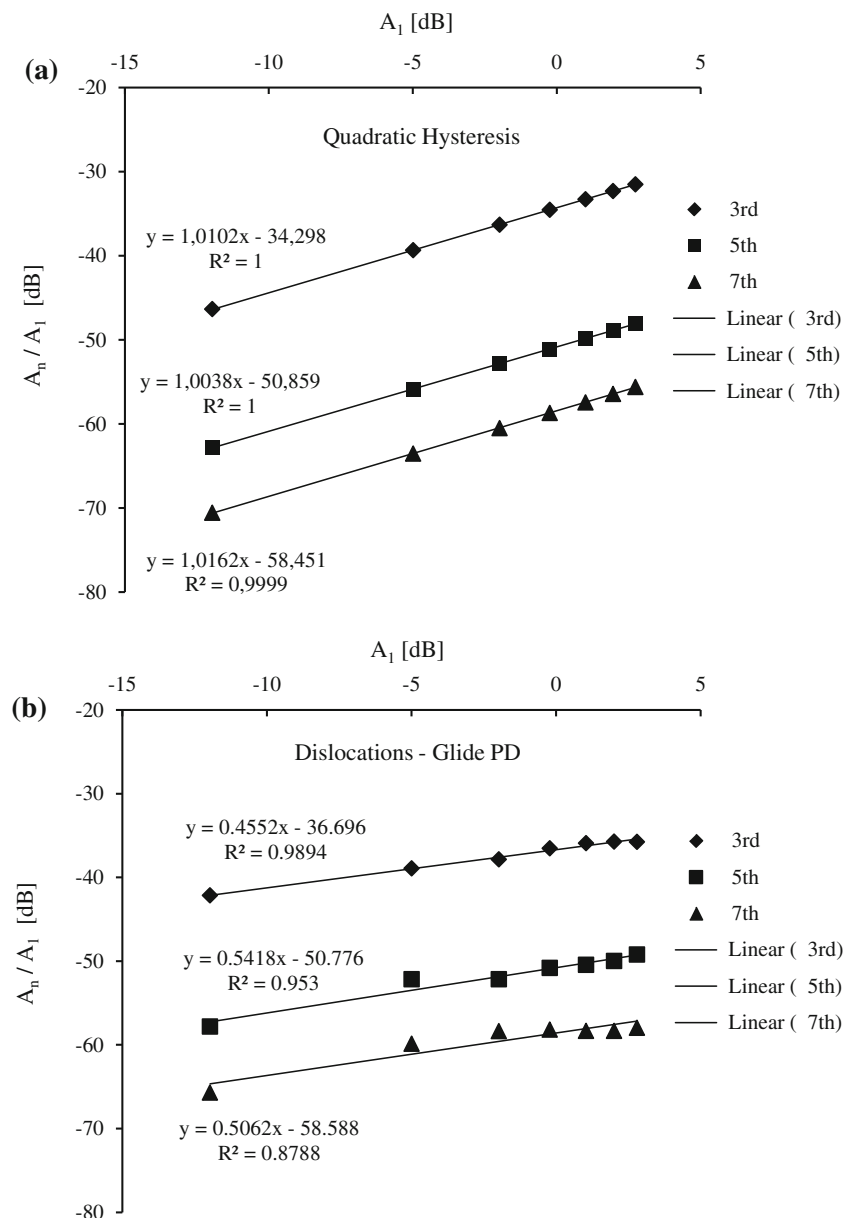
Scalerandi et al. [18] commented that, when the nonlinear signature employed in the scaling subtraction method is reported against the amplitude of the nonlinear response on a log-log scale, the slope of the apparently linear dependence of the former on the latter may be used to differentiate forms of damage of diverse physical origin. The present models can be used to produce similar plots for the fundamental components and its higher harmonics. However, notice must be taken of the fact that the plots produced by the scaling subtraction method, since they are derived directly from time-domain signals, include the effect of the phase shift caused by the amplitude-dependent softening induced by damaged. The plots produced with the models presented in this work, on the other hand, use the magnitude of Fourier components of the time-domain signals, and, thus, do not account for the latter effect. For damage described by quadratic hysteresis,

the slope of the theoretical data interpolation is equal to one in all cases reported in Fig. 7a. For damage in the form of distributions of dislocations, no linear fit of the data in Fig. 7b can be conceived, and their quality worsens with increasing harmonic order, although they all approach a value of 0.5. As the present model and additional results in [13] show, the slope of these lines appears to be sensitive to both the physical nature of damage, which is encoded in the rheological model behind the constitutive relation, and to the distribution of the critical stress, $\varphi(\sigma_{cr})$, which, in principle, may be a property shared by other forms of damage. This situation is typical of wave phenomena where a probing wave interacts with distributions of scatterers. For instance, the nonlinear response of interfaces formed by rough solid surfaces in contact to an inspecting ultrasonic wave is the result of two contributions, the first one being the nonlinear behavior of the contacts under compression, and the second one being due to the distributions of the asperities height. In conclusion, although the present theoretical results do not provide conclusive evidence against the method proposed by Scalerandi et al. [18] and references therein, they suggest that a confident use of the latter requires two major points to be clarified. The first one concern the restoration of the linear dependence in Fig. 7a, which is so clearly violated by the results related to the interaction between dislocations and point defects. A possible solution of this conflict may reside in the effect of the phase variation discussed above. Second, evidence should be given which proves that the linear stress dependence on a log-log scale is a consequence of the nonlinear mechanism in itself and not of the distribution of its activation energy. In the opposite case, different damage distributions of defects of identical physical nature would be assigned different exponents.

4.2 Non-Uniform Distribution

Damage evolves from specific locations within a structure, increasing in severity and spatial extent. To exemplify the effect of damage localization on the nonlinear response of a bar under forced harmonic oscillations, four rectangular distributions with the same area have been considered. In Fig. 8, the distribution labeled D1 is the uniform distribution used in the previous section, and D2, D3, and D4 are distributions having the same area as D1, but width equal to 0.5, 0.2, and 0.05L, respectively. Figure 9 shows the effect of varying the width of the distribution maintaining its area constant on the relative variation of the amplitude of the fundamental harmonic component for both types of damage. In both cases, there is a detectable increase of the nonlinear attenuation following the reduction of the distribution width. This behavior is particularly pronounced at the early stages of damage localization. The reason for the strengthening of the effect when damage is highly localized

Fig. 7 Stress dependence of the first three higher harmonic components for **a** quadratic hysteretic damage, and **b** distributions of dislocations. Best linear fit are shown together with the corresponding equations and R values. Stress values are given in units of MPa



is, in part, due to the increase of the average value of the stress over the extent of the damage distribution. This quantity varies between 60% of the maximum amplitude, Σ , for the uniform distribution, D1, to 93% of the same amplitude for D4. Note that the values of $(1 - A_1/A_{Lin})$ for D1 and D4 differ by a factor about 2.5. This variation cannot be accounted for by that of the average value of the stress amplitude. Another and definitely more relevant contribution to this difference is due to interference among the non-linear sources of higher harmonics [see Eq. (23)] which is less destructive when the location of the sources is more concentrated.

To investigate the relative contribution of these two causes, a simulation was carried out using distributions of damage

consisting of two rectangular regions of width $0.1L$ each, placed in symmetrical positions with respect to the center of the bar, and with their centers at relative distance, d , varying from 0.1 to $0.9L$. Damage was of the type described by quadratic hysteresis. For each distribution, the value of the relative variation of the stress amplitude was calculated twice. The first time, the strength of the applied source was equal to $\Sigma = 2$ kPa for all distributions. The second time, the strength of the source was modified so that the stress acting on the damage had strength equal to its value at the center of the bar when the distance between the two regions was $d = 0.1L$. Figure 10 shows the results of these simulations. The relative change of the amplitude of the fundamental harmonics appears to decrease as d increases at a similar rate in the two

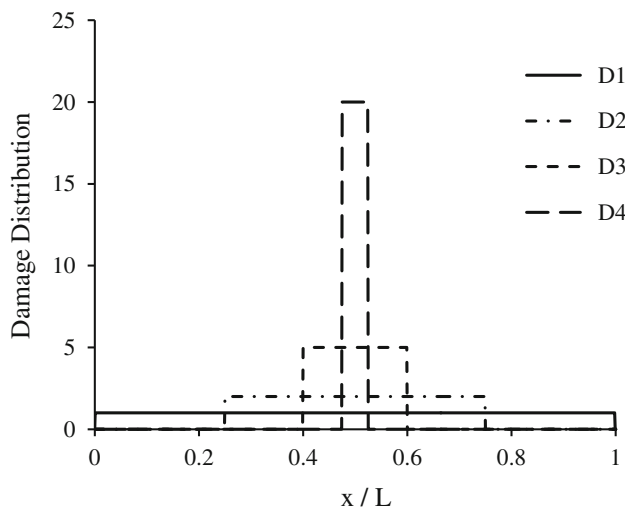


Fig. 8 Four examples of rectangular distributions having the same area. Distribution D1 is constant over the bar, while the width of D2, D3, and D4, are 0.5, 0.2, and 0.05 L, respectively

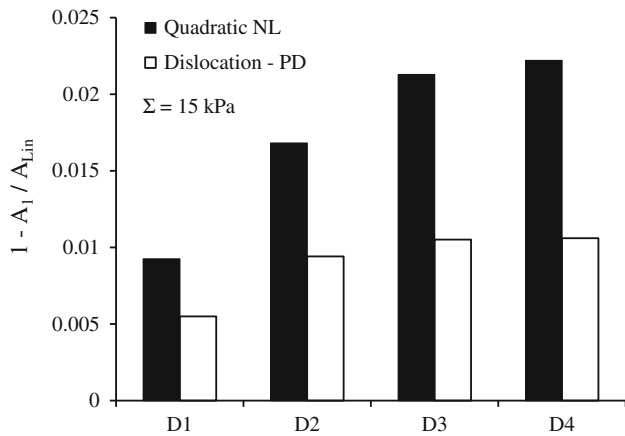


Fig. 9 Relative amplitude variation of the fundamental component for four rectangular distributions of damage of decreasing width and same area. *Black bars* refer to damage described by quadratic nonlinearity, *white bars* to dislocations interacting with point defects

cases. This result shows that maintaining the stress constant over the region of damage does not significantly affect the nonlinear attenuation. On the other hand, the geometry of the damage distribution is proven to be a key factor in controlling the magnitude of nonlinear attenuation produced by localized damage when the fundamental mode of the bar is excited.

Nonlinear attenuation of the fundamental component depends on the physical parameters characterizing the system’s nonlinearity besides the distribution width. Therefore, when considering the problem of assessing the spatial extent of the distribution, it may be of interest to investigate whether other acoustic properties of the nonlinear response of the distributions at hand may be of help to this end. Figure (11a, b)

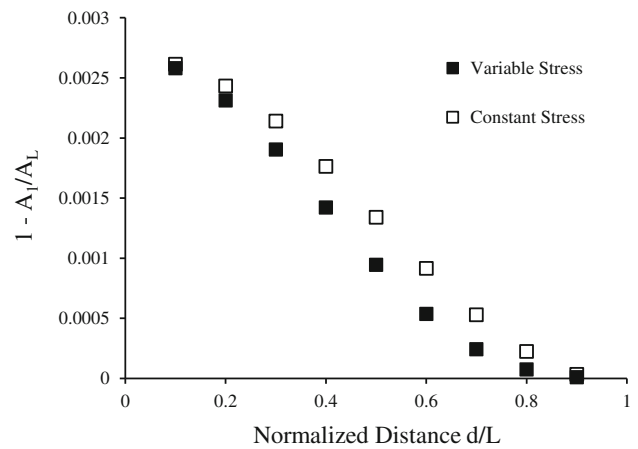


Fig. 10 Relative amplitude variation of the fundamental component produced by localized damage regions in symmetrical position with respect to the center of the bar and at distance d . Data have been calculated for a stress field generated by a source of strength $\Sigma = 2$ kPa (*black symbols*), or by sources producing the same stress at the damage location (*open symbols*)

shows the ratio between the amplitude of the third and the n -th higher harmonic component, with $n = 5, 7, 9, 11$, generated by (a) damage leading to quadratic hysteresis, and (b) dislocations, all having spatial distributions D1, D2, D3, and D4 shown in Fig. 8. Recall that all higher harmonics have the same dependence on the source amplitude. In particular, in the case of quadratic hysteresis higher harmonics are proportional to Σ^2 . Therefore, when their ratio is considered, any effect of the source’s amplitude is eliminated. For dislocations interacting with point defects, there remains an effect of the source amplitude which is mediated by the fraction of depinned dislocations. The latter can still be regarded as a property of the material system rather than of the inspection technique. In other words, the magnitude of these differences depends on properties that either are entirely intrinsic to the distributions in the case of quadratic hysteresis, or, at most, are affected by the excitation amplitude only through some intrinsic properties of the damage of interest, such as the distribution of the critical stress, σ_{cr} [see Eq. (7)]. Figure 11 illustrates that, disregarding minor variations between the two models, the uniform distribution consistently generates harmonics higher than the third with less efficiency. In other words, the efficiency of the generation of higher harmonics increases with the concentration of damage. It is plausible, therefore, to consider these or similar data as signatures of the distributions themselves, and to use them for discrimination purposes in a Bayesian strategy of model’s selection as discussed by Bretthorst [19]. In this context, it is also clear that any prior information obtained from other features of the bar’s nonlinear response may be of considerable help to characterize the extent of the region of damage. For instance, having identified the nature of damage affecting the mater-

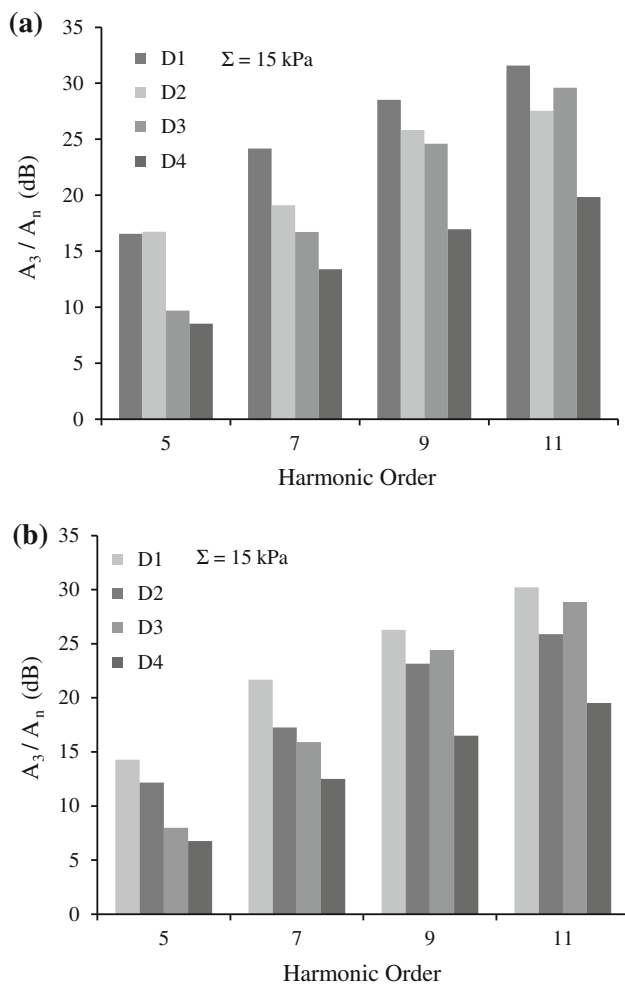


Fig. 11 Harmonic amplitudes normalized with respect to the amplitude of the third harmonic component for damage **a** represented by a quadratic hysteresis, **b** distribution of dislocations. The strength of the source is $\Sigma = 15$ kPa

ial via the dependence of the nonlinear attenuation of the fundamental component, the possible models to be tested could be reduced to those associated to that type of damage.

In this investigation, the nonlinear response of a bar with hysteretic damage has been predicted also assuming spatial distributions that are exponential or Gaussian. The results of these simulations, which are not reported here explicitly, indicate that among three distributions having the same area, the rectangular one generates the strongest nonlinearity, while the Gaussian is the least responsive of the three. Finally, simulations aiming at assessing the effect of location of a narrow region of damage along the bar have led to the same conclusions at which other investigations have arrived earlier (see, for example, Gliozzi et al. [2]). That is to say, locations that are symmetric with respect the center of the bar produce nonlinear responses which are identical for all practical purposes, the reason for it being the symmetry of the exciting stress field along the bar.

5 Concluding Remarks

Attempts at linking the acoustic nonlinear response of a material to realistic mechanisms responsible for damage at the micro/mesoscale are still limited in number and accuracy. As mentioned in the introduction while reporting on the results by Gliozzi et al. [2], researchers active in this area (see also Renaud et al. [20]) seem to share the conviction that deeper understanding of the actual physical mechanisms affecting the nonlinear dynamic response of damaged materials is necessary to further the application of nonlinear inspection methods to problems of practical relevance. Part of this larger problem lies also in the lack of convincing mathematical models connecting various forms of damage to the acoustic nonlinearity manifested by these materials.

The long-term goal of the present effort is to develop a mathematical framework which allows the nonlinear response elicited in a resonance test and caused by different forms of material damage to be predicted, and, possibly, differentiated. In this communication a theoretical model has been presented which describes the longitudinal forced vibrations of a bar affected by hysteretic damage over a limited region of the bar. The mathematical model sets no constraints on the geometry of the damage distribution, and shows how the spatial component of the solution is modified by this factor. Two constitutive relationships have been considered. In the first one, hysteresis has a quadratic dependence on the instantaneous stress. This model has been widely used in previous studies for its ability to reproduce the most characteristic trends shown by experimental results. In this work, it plays the role of reference model. The second constitutive relationship describes the interactions of dislocations with point defects distributed along their glide planes. This is a realistic mechanism leading to hysteresis between macroscopic strain and stress.

The equation of motion has been solved by means of a perturbation technique which allows the effect of damage on both the fundamental component of the nonlinear response, and the generation of higher harmonics to be predicted. Damaged-induced material softening is a common manifestation to both forms of damage. However, the strong resemblance between the two hysteresis cycles notwithstanding, the nonlinear attenuation due to a distribution of dislocations is shown to be characterized by a behavior which markedly departs from that produced by quadratic hysteresis. This departure can be observed when the amplitude of the excitation ranges over values sufficiently large to cause depinning of a sizeable fraction of dislocations from the point defects with which they interact. Only for values of the amplitude of the excitation much smaller than the width of the distribution in Eq. (7), the predictions of the two models tend to agree, at least qualitatively. Consistently with the similarity between the two hysteresis cycles, on the other hand, the

spectral responses of two distributions of damage, which are spatially identical but of different physical nature, strongly resemble each other.

Several additional models of damage have been mentioned in the literature [7] for which constitutive relationships like Eq. (8) should be developed. Eventually, these might be modified to describe not only the mechanical properties of the system in an equilibrium state, but also its possible paths to equilibrium. A noteworthy application of this development would be to provide credible explanations for the conditioning effect. To this day, however, the mathematical formulation of the dynamics leading a material with defects at the micro/mesoscale to thermodynamic equilibrium seems to be a subject requiring investigations on their own. In this context, therefore, it seems reasonable to prioritize the identification of those physical mechanisms that are responsible for the variety of already documented acoustic responses of material nonlinearity under approximately equilibrium conditions (see Renaud et al. [20], for example), leaving problems of considerable greater complexity to be tackled in later studies.

In the greatest number of investigations on the nonlinear response of a material to an external disturbance, the quantity which is used as the independent variable is the maximum value of the strain amplitude. Here, stress, and not strain, has been considered as the independent variable. This choice is dictated by the fact that stress, not strain, is the physical quantity, which is under direct control of the experimenter, affecting the material response. In fact, stress is continuous across the interface between source and sample, while strain depends on the boundary condition on the displacement at the interface between source and material. With that said, for a given experimental setting and nonlinear damage far from levels producing catastrophic failure, the difference between using stress and strain as independent variable, although undesirable in reporting experimental results, should not be expected to produce major distortions in the representation of the results and in their interpretation.

Finally, for a given type of damage, spectral features have been identified which a Bayesian procedure for model selection could be used to discriminate distributions of damage of different spatial extent. To this end, however, identification of the physical nature of damage is required. In this context, the relevance of prior independent information, possibly derived from additional features of the nonlinear response of the material, has been stressed.

References

1. Lyakhovskiy, V., Hamiel, Y., Ben-Zion, Y.: A non-local viscoelastic damage and dynamic fracturing. *J. Mech. Phys. Solids* **59**, 1752–1776 (2011)
2. Gliozzi, A.S., Nobili, M., Scalerandi, M.: Modelling localized nonlinear damage and analysis of its influence on resonance frequencies. *J. Phys. D* **39**, 3895–3903 (2006)
3. Van Den Abeele, K., Schubert, F., Aleshin, V., Windels, F., Carmeliet, J.: Resonant bar simulations in media with localized damage. *Ultrasonics* **42**, 1017–1024 (2004)
4. Windels, F., Van Den Abeele, K.: The influence of localized damage in a sample on its resonance spectrum. *Ultrasonics* **42**, 1025–1029 (2004)
5. Van Den Abeele, K.: Multi-mode nonlinear resonance ultrasound spectroscopy for defect imaging: an analytical approach for the one-dimensional case. *J. Acoust. Soc. Am.* **122**, 73–90 (2007)
6. Guyer, R.A., Johnson, P.A.: *Nonlinear mesoscopic elasticity*. Wiley, Berlin (2009)
7. Ostrovsky, L.A., Johnson, P.A.: Dynamic nonlinear elasticity in geomaterials. *Rivista del Nuovo Cimento* **24**, 1–46 (2001)
8. Aleshin, V., Van Den Abeele, K.: Microcontact-based theory for acoustics in microdamaged materials. *J. Phys. Mech. Solids* **55**, 366–390 (2007)
9. Lyakhovskiy, V., Hamiel, Y., Ampuero, J.-P., Ben-Zion, Y.: Non-linear damage rheology and wave resonance in rocks. *Geophys. J. Int.* **178**, 910–920 (2009)
10. Gremaud, G.: Dislocations—point defects interactions. *Mater Sci Forum* **366–368**, 178–246 (2001)
11. Pecorari, C., Mendelsohn, D.A.: Nonlinear forced vibrations of a hysteretic bar: revisited. *Wave Motion* **50**, 127–134 (2013)
12. Pecorari, C.: Nonlinear interaction of plane ultrasonic waves with an interface between rough surfaces in contact. *J. Acoust. Soc. Am.* **113**, 3065–3072 (2003)
13. Pecorari, C.: Modeling the acousto-elastic hysteretic of dry Berea sandstone. Submitted for publication.
14. Renaud, G., Rivière, J., Bas, P.-Y., Johnson, P.A.: Hysteretic nonlinear elasticity of Berea sandstone at low-vibrational strain revealed by dynamic acousto-elastic testing. *Geophys. Res. Lett.* **40**, 715–719 (2013)
15. Scalerandi, M., Gliozzi, A.S., Bruno, C.L.E., Masera, D., Bocca, P.: A scaling method to enhance detection of a nonlinear elastic response. *Appl. Phys. Lett.* **92**, 101912 (2008)
16. Bruno, C.L.E., Gliozzi, A.S., Scalerandi, M., Antonaci, P.: Analysis of elastic nonlinearity using the scaling subtraction method. *Phys. Rev. B* **79**, 064108 (2009)
17. Riviere, J., Renaud, G., Guyer, R.A., Johnson, P.A.: Pump and probe waves in dynamic acousto-elasticity: comprehensive description and comparison with nonlinear elastic theories. *J. Appl. Phys.* **114**, 054905 (2013)
18. Scalerandi, M., Griffa, M., Antonaci, P., Wyrzykowski, M., Lura, P.: Nonlinear elastic response of thermally damaged consolidated granular media. *J. Appl. Phys.* **113**, 154902 (2013)
19. Bretthorst, G.L.: An introduction to model selection using probability theory as logic. In: Heidbreder, G.R. (ed.) *Maximum entropy and Bayesian methods*, pp. 1–41. Kluwer Academic Publishers, Dordrecht (1996)
20. Renaud, G., Le Bas, P.-Y., Johnson, P.A.: Revealing highly complex elastic nonlinear (anelastic) behavior of earth materials applying a new probe: dynamic acoustoelastic testing. *J. Geophys. Res.* **117**, B06202 (2012)